Flavin Adenine Dinucleotide Structural Motifs: From Solution to Gas Phase

Juan Camilo Molano-Arevalo,[†] Diana R. Hernandez,[†] Walter G. Gonzalez,[†] Jaroslava Miksovska,[†] Mark E. Ridgeway,[‡] Melvin A. Park,[‡] and Francisco Fernandez-Lima*[,†,§]

[†]Department of Chemistry and Biochemistry, Florida International University, Miami, Florida 33199, United States
[‡]Bruker Daltonics Inc., Billerica, Massachusetts 01821, United States
[§]Biomolecular Sciences Institute, Florida International University, Miami, Florida 33199, United States

S *Supporting Information*

ABSTRACT: Flavin adenine dinucleotide (FAD) is involved in important metabolic reactions where the biological function is intrinsically related to changes in conformation. In the present work, FAD conformational changes were studied in solution and in gas phase by measuring the fluorescence decay time and ion-neutral collision cross sections (CCS, in a trapped ion mobility spectrometer, TIMS) as a function of the solvent conditions (i.e., organic content) and gas-phase collisional partner (i.e., N_2 doped with organic molecules). Changes in the fluorescence decay suggest that FAD can exist in four conformations in solution, where the abundance of the extended conformations increases with the organic content. TIMS-MS experiments showed that FAD can exist in the gas phase as deprotonated (M = $C_{27}H_{31}N_9O_{15}P_2$) and protonated forms (M = $C_{27}H_{33}N_9O_{15}P_2$) and that multiple conformations (up to 12) can be observed as a function of the starting solution for the $[M + H]^+$ and $[M + Na]^+$ molecular ions. In addition, changes in the relative abundances of the gas-phase structures were observed from a "stack" to a "close" conformation when organic molecules were introduced in the TIMS cell as collision partners. Candidate structures optimized at the DFT/B3LYP/6-31G(d,p) were proposed for each IMS band, and results showed that the most abundant IMS band corresponds to the most stable candidate structure. Solution and gas-phase experiments suggest that the driving force that stabilizes the different conformations is based on the interaction of the adenine and isoalloxazine rings that can be tailored by the "solvation" effect created with the organic molecules.
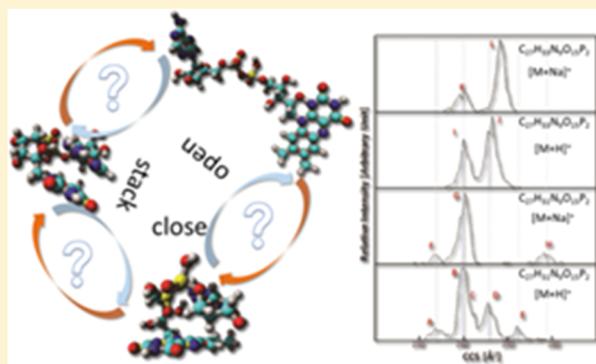
Flavin adenine dinucleotide (FAD) is involved in multiple metabolic reactions. Its primary role is being a cofactor necessary for the activity of numerous flavoproteins, which play an important role in electron transport pathways in living systems like respiration,[1] photosynthesis,[2,3] DNA repair,[4,5] and photoreceptors and nitrogen fixation.[6] Since Weber[7] reported a weakness in the fluorescence of FAD in comparison with the fluorescence of free riboflavin, a number of studies has proposed the existence of at least two conformers for FAD in solution.[8,9] One "stack" conformer exhibits a quenching of fluorescence, which presents a $\pi-\pi$ interaction between aromatic rings and intramolecular hydrogen bonds that stabilizes the adenine moiety and isoalloxazine ring,[10,11] which might contribute to 80% of the molecules of FAD in solution.[12] Additionally, an "open" conformer does not present quenching of the fluorescence.[7,13] Even though the existence of an "open" and a "stack" conformation is generally accepted, little is known about the structural details and the conformational space of FAD. Studies on free riboflavin and the adenosine derivative 5′-bromo-5′-deoxyadenosine using crystallographic methods have shown an average structure of the $\pi-\pi$ systems.[14] Different models for the interaction between the flavin and adenine moieties have been proposed on the basis of NMR studies.[11,15−18] However, all NMR studies presented the complication of intermolecular stacking between the flavin complexes at millimolar concentrations.

During the last decades, ion mobility spectrometry (IMS) combined with molecular dynamic simulations has proven to be a versatile technique for the analysis of intermediate and equilibrium structures of biomolecules enabling the correlation of ion-neutral, collision cross sections (CCS) with candidate structures.[19−24] In particular, it has been shown that using soft ionization techniques (e.g., electrospray ionization, ESI[25]) the evaporative cooling of the solvent leads to a freezing of multiple conformations, which has permitted the study of the conformational space dependence on the solvent conditions (e.g., native vs denatured), bath gas collision partner, and temperature.[26−37]

With the recent introduction of trapped ion mobility spectrometry coupled to mass spectrometry (TIMS-MS),[38,39] we have shown that high mobility separations (R = 100−250) can be routinely achieved.[40] In particular, we have shown that the study of biomolecules traditionally named "unstructured" by NMR and XRD is feasible due to the ability to measure multiple conformations at a given time and to perform kinetic studies of conformational interconversion as a way to elucidate folding/unfolding pathways.[41,42]

In the present work, the conformational space of FAD in solution phase and in gas phase as a function of the solution composition was studied using a combination of TIMS-MS, fluorescence time decay, and molecular dynamics (MD) simulations. We present evidence that FAD $[M + H]^+$ and $[M + Na]^+$ molecular ions observed during ESI can be deprotonated and protonated, which leads to multiple stable conformations (totaling 12 IMS bands) whose relative abundance can be tailored by the solvent conditions and the gas-phase collision partner. Special attention was given to the interrelation between the MD and IMS data, and candidate structures for each IMS band are proposed.

■ METHODS

Materials and Reagents. Flavin adenine dinucleotide disodium salt hydrate (F6625) powder was purchased from Sigma-Aldrich (St. Louis, MO) and used as received. All solvents and ammonium acetate salts used in these studies were analytical grade or better and purchased from Fisher Scientific (Pittsburgh, PA). A stock solution was prepared in 10 mM ammonium acetate, and aliquots were diluted to a final concentration of 1, 5, and 10 μM in 70:30, 50:50, and 30:70 (v/v) water−methanol/ethanol solutions. A Tuning Mix calibration standard (TuneMix, G24221A) was purchased from Agilent Technologies (Santa Clara, CA) and used as received. Details on the Tunemix structures (e.g., m/z = 322, K_0 = 1.376 cm^2 V^{-1} s^{-1} and m/z = 622, K_0 = 1.013 cm^2 V^{-1} s^{-1}) can be found elsewhere.[40,43] All experiments were performed in triplicates.

Trapped Ion Mobility Spectrometry−Mass Spectrometry Separation. Details regarding the TIMS operation and specifics compared to traditional IMS can be found elsewhere.[38−42] Briefly, in TIMS mobility, separation is based on holding the ions stationary using an electric field against a moving gas. The separation in a TIMS device can be described by the center of the mass frame using the same principles as in a conventional IMS drift tube.[44] Since mobility separation is related to the number of ion-neutral collisions (or drift time in traditional drift tube cells), the mobility separation in a TIMS device depends on the bath gas drift velocity, ion confinement, and ion elution parameters. The reduced mobility, K_0, of an ion in a TIMS cell is described by

$$K_0 = \frac{v_g}{E} = \frac{A}{(V_{elution} - V_{base})} \quad (1)$$

where v_g, E, $V_{elution}$, and V_{base} are the velocity of the gas, applied electric field, elution and base voltages, respectively. The constant A can be determined using calibration standards of known reduced mobilities. In TIMS operation, multiple geometric isomers/conformers are trapped simultaneously at different E values resulting from a voltage gradient applied across the TIMS tunnel. After thermalization, geometrical isomers/conformers are eluted by decreasing the electric field

in stepwise decrements (referred to as the "ramp"). Each isomer/conformer eluting from the TIMS cell can be described by a characteristic voltage (i.e., $V_{elution} - V_{base}$). Eluted ions are then mass analyzed and detected by a maXis impact Q-ToF mass spectrometer (Bruker Daltonics Inc., Billerica, MA).

In a TIMS device, the total analysis time can be described as

$$\text{total IMS time} = T_{trap} + (V_{elution}/V_{ramp}) \times T_{ramp} + \text{ToF}$$

$$= T_o + (V_{elution}/V_{ramp}) \times T_{ramp} \quad (2)$$

where T_{trap} is the thermalization/trapping time, ToF is the time after the mobility separation, and V_{ramp} and T_{ramp} are the voltage range and time required to vary the electric field, respectively. The elution voltage can be experimentally determined by varying the ramp time for a constant ramp voltage. This procedure also determines the time ions spend outside the separation region T_o (e.g., ion trapping and time-of-flight).

The TIMS funnel is controlled using in-house software, written in National Instruments Lab VIEW, and synchronized with the maXis Impact Q-ToF acquisition program.[38,39] TIMS separation was performed using nitrogen as a bath gas at ca. 300 K, and the gas flow velocity was controlled by the pressure difference between entrance funnel P_1 = 2.6 mbar and the exit funnel P_2 = 1.0 mbar. P_1 and P_2 values were held constant for all experiments. Dopant additives were introduced at the entrance of the tunnel region of the TIMS analyzer and monitored with an external capacitance gauge from MKS instruments (Andover, MA). Methanol, ethanol, and acetone were used as dopant additives and introduced through a 1 mm i.d. aperture at 10 mbar. The same RF (880 kHz and 200Vpp) was applied to all electrodes including the entrance funnel, the mobility separating section, and the exit funnel. An electrospray ionization source (ESI Apollo II design, Bruker Daltonics, Inc., MA) was used for all the analyses. The TIMS cell was operated using a fill/trap/ramp/wait sequence of 10/10/50−500/50 ms. Average mobility resolution at 10/10/500/50 was 160−190.

Reduced mobility values (K_0) were correlated with CCS (Ω) using the equation:

$$\Omega = \frac{(18\pi)^{1/2}}{16} \frac{z}{(k_B T)^{1/2}} \left[\frac{1}{m_I} + \frac{1}{m_b} \right]^{1/2} \frac{1}{K_0} \frac{1}{N^*} \quad (3)$$

where z is the charge of the ion, k_B is the Boltzmann constant, N^* is the number density, and m_I and m_b refer to the masses of the ion and bath gas, respectively.[44]

Fluorescence Decay Analysis. Fluorescence decay experiments were performed on FAD as a function of the solvent conditions using a ChronosFD spectrofluorometer (ISS, Champaign, IL) in the frequency domain mode. A 10 μM FAD solution was excited using a 470 nm laser diode, and fluorescent emission was collected using 500 and 650 nm long and short pass filters, respectively (Andover, Salem, NH). A rhodamine B water solution was used for lifetime calibration (τ =1.7 ns).[45] Polarizers were set at magic angle configuration. The fluorescence decay lifetimes were recovered by a nonlinear fit of the data using a triple exponential decay using GlobalWe software (Laboratory of Fluorescence Dynamics, Irvine, CA).

Theoretical Calculations. A pool of candidate structures were proposed for each molecular ion observed in the TIMS-MS experiments. The initial pool of candidate structures was obtained using serial molecular dynamics simulations of

annealing and geometry optimization cycles in a NVT thermostat (equivalent to the approach described in ref 31) using AMBER03 force field in YASARA software. In particular, the NVT thermostat was set to recreate the TIMS cell experiment; the simulation box contained the molecular ion of interest with bath and dopant gas molecules. Final structures were optimized at the DFT/B3LYP/6-31G(d,p) level using Gaussian software.[46] Vibrational frequencies were calculated to guarantee that the optimized structures correspond to a real minima in the energy space, and zero-point energy corrections were applied to calculate the relative stability between the structures for each FAD form (i.e., $[M + H]^+$ and $[M + Na]^+$, $M = C_{27}H_{33}N_9O_{15}P_2$ and $[M + H]^+$ and $[M + Na]^+$, $M = C_{27}H_{31}N_9O_{15}P_2$). During the IMS experimental conditions (i.e., 300 K), the structures may interconvert and transitions states (and energy barriers) were not calculated in the present work. However, the observation of multiple IMS bands suggests that multiple local minima exist which translates into the existence of multiple conformations. Theoretical ion-neutral collision cross sections were calculated using MOBCAL version for helium[47,48] and nitrogen,[49,50] as a bath gas at ca. 300 K. It should be noted that the MOBCAL version for nitrogen was used assuming the similarity of the molecules to those used to develop the Lennard-Jones potential at 300 K in refs 49 and 50; for other molecules, alternatives methods are encouraged.[51] Partial atomic charges were calculated using the Merz–Singh–Kollman scheme constrained to the molecular dipole moment.[52,53] All optimized geometries and partial atomic charges used in the MOBCAL input files are provided in the Supporting Information.

■ RESULTS AND DISCUSSION

The MS analysis of FAD shows that four molecular ions are produced by the ESI source, independent of the water–organic content ratio (Figure 1). The most abundant $[M + H]^+$ and $[M + Na]^+$ molecular ions correspond to the protonated form of FAD ($M = C_{27}H_{33}N_9O_{15}P_2$), while similar molecular ions were observed for the deprotonated form ($M = C_{27}H_{31}N_9O_{15}P_2$). This result is consistent with previously reported MS experiments (KNA00612 record from www.massbank.jp). Taking advantage of the high resolution of the MS spectrometer ($R > 30–40k$), mass signals were isolated ($\Delta m/z < 1$ Da, monoisotopic peak) and mobility experiments were performed for each molecular ion as a function of the solvent condition and bath gas composition.

Mobility experiments were performed as a function of the organic content in the starting solutions (e.g., water–ethanol/methanol content) using nitrogen as a bath gas (Figure 2). Inspection of the mobility spectrum showed that multiple conformations exist as a function of the solvent conditions (labels A–L). Ion-neutral CCSs were determined for all molecular ions observed using Tuning Mix species as external calibrants (Table 1). Major differences in the relative abundances were not observed as a function of the starting solution (e.g., organic content) and the IMS trapping time. This suggests that all structures formed during the ESI process (labeled A–L) are stable in the TIMS experiments time scale (50–2000 ms). No changes in the CCS values were observed as a function of the starting solutions (e.g., water–ethanol/methanol content) which suggest that the observed IMS bands correspond to different conformations of FAD and not to organic solvent clustering onto the molecular ions.
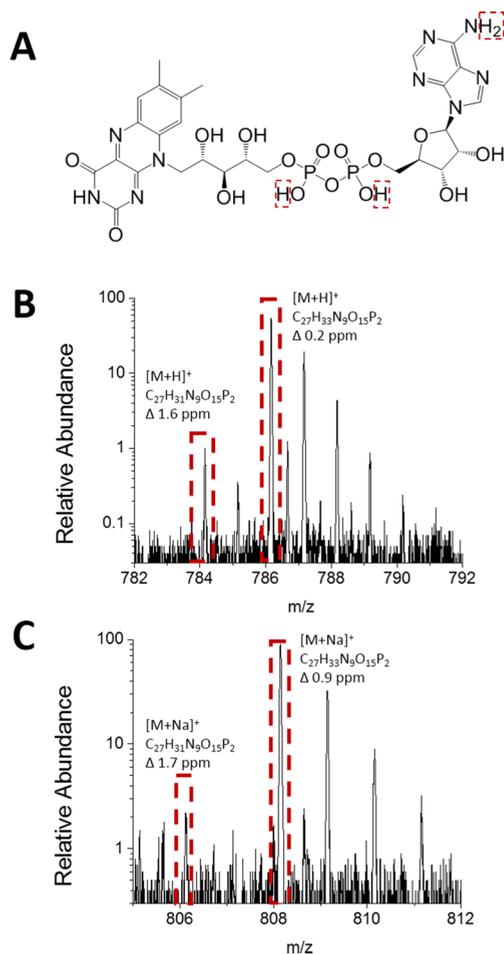

Figure 1. Structure and typical MS spectra for the deprotonated ($M = C_{27}H_{31}N_9O_{15}P_2$) and protonated ($M = C_{27}H_{33}N_9O_{15}P_2$) FAD forms. Monoisotopic peaks of the $[M + H]^+$ and $[M + Na]^+$ molecular ions used in the mobility analysis are highlighted with a dashed rectangle.

The conformational heterogeneity of FAD in solution was characterized by measuring the FAD lifetime in water–ethanol/methanol mixtures using frequency domain fluorescence spectroscopy (Figure 3). The data were analyzed using the triple exponential decay model, and the results are summarized in Table 2. Three distinct components were resolved: a fast component of ~270 ps and two nanosecond components with the lifetimes of 2.43 and 4.6 ns in water. The observed lifetimes are in agreement with previous reports of FAD emission lifetimes in water and water–ethanol mixtures.[54,55] The fast decaying component of ~270 ps is attributed to a "closed" FAD conformation with relatively weak interactions between the isoalloxazine and adenine ring that lead to a less efficient intramolecular transfer between the heteroaromatic groups.[7,13] The nanosecond lifetimes of ~2.5 and ~4.6 ns correspond to the "partially open" and "open" FAD conformation, respectively. In the "open" conformation, the distance between the isoalloxazine and adenine ring was proposed to be approximately 16 Å, preventing an efficient quenching of the flavine emission.[56] An additional lifetime of ~10 ps (not resolved in our measurements) was identified in femtosecond fluorescence lifetime studies and attributed to a "stack" conformation with the intramolecular distance between the heteroaromatic groups of ~4 Å.[54] Inspection of Figure 3 and Table 2 shows that the increase in the organic content (i.e., methanol/ethanol) leads to
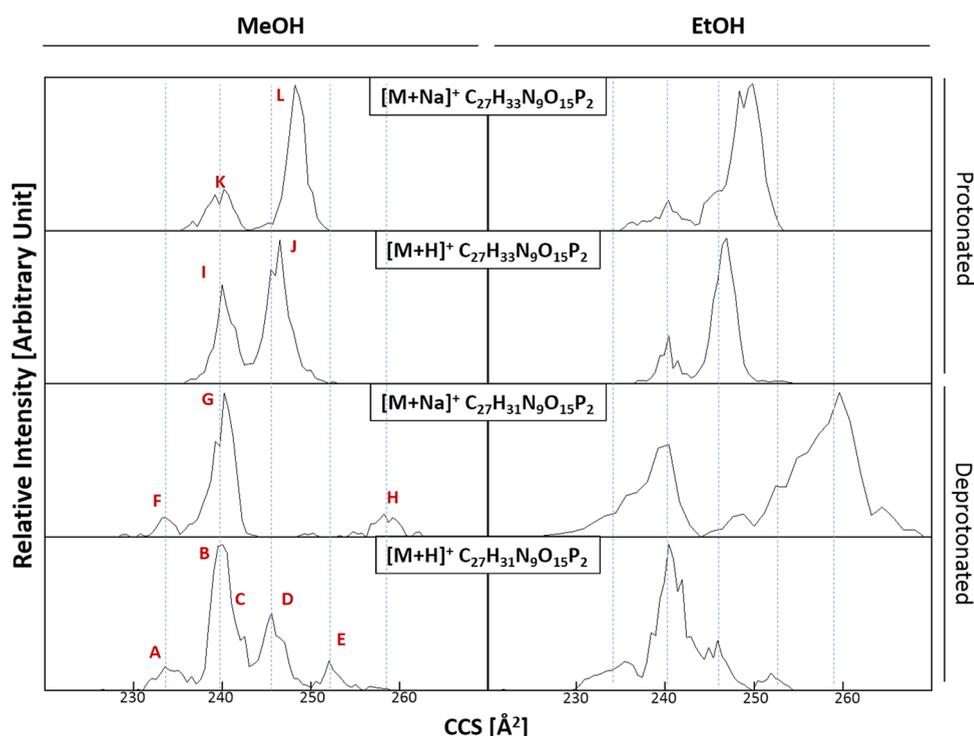
Figure 2. Typical TIMS spectra as a function of the organic content for the $[M + H]^+$ and $[M + Na]^+$ molecular ions of the deprotonated (M = $C_{27}H_{31}N_9O_{15}P_2$) and protonated (M = $C_{27}H_{33}N_9O_{15}P_2$) FAD forms.

Table 1. Experimental and Theoretical Ion-Neutral Collision Cross Section for the $[M + H]^+$ and $[M + Na]^+$ Molecular Ions of the Deprotonated (M = $C_{27}H_{31}N_9O_{15}P_2$) and Protonated (M = $C_{27}H_{33}N_9O_{15}P_2$) FAD Forms[a]

conformation		experimental CCS [Å²]	d [Å]	MOBCAL He			MOBCAL N₂	
				PA	EHS	TM	TM (B3LYP/6-31G(d,p) with charges)	relative energy [kcal/mol]
$[M + H]^+$ $C_{27}H_{31}N_9O_{15}P_2$ m/z = 784.14 Δ 1.6 ppm	A	235	4.318	159.79	174.53	159.15	238.31	27.23
	B	240	4.831	160.73	175.18	160.42	240.11	0
	C	242	5.122	162.16	176.32	161.97	244.85	24.86
	D	246	5.244	162.64	177.77	161.99	247.92	20.92
	E	253	5.915	164.88	179.08	162.46	252.79	41.61
$[M + Na]^+$ $C_{27}H_{31}N_9O_{15}P_2$ m/z = 806.13 Δ 0.2 ppm	F	233	5.204	159.58	173.20	159.05	234.28	16.93
	G	240	5.570	161.11	176.99	162.10	241.53	0
	H	259	5.993	163.96	179.18	164.61	258.08	4.329
$[M + H]^+$ $C_{27}H_{33}N_9O_{15}P_2$ m/z = 786.15 Δ 1.7 ppm	I	240	4.969	165.36	181.55	162.81	241.26	0
	J	246	5.102	169.50	186.66	167.02	247.51	31.43
$[M + Na]^+$ $C_{27}H_{33}N_9O_{15}P_2$ m/z = 808.14 Δ 0.9 ppm	K	240	5.027	164.64	180.06	168.46	242.83	0
	L	248	5.382	166.50	180.80	169.11	248.64	15.07

[a]Energies were calculated at level B3LYP/6-31G(d,P) and shown relative to the most stable isomer. The distances (d) between the isoalloxazine and adenine ring are shown for each conformation.

the increase in the fraction of the open conformation that is characterized by ∼4.6 ns lifetime; this is in good agreement with previous experiments where the increase in the dielectric constant of medium altered the population of "stack" and "open" conformations of FAD.[54,56]

Candidate structures were proposed for IMS bands A−L (Figure 4). For the $[M + H]^+$ and $[M + Na]^+$ molecular ions observed of the deprotonated (M = $C_{27}H_{31}N_9O_{15}P_2$) and protonated (M = $C_{27}H_{33}N_9O_{15}P_2$) forms of FAD, the lowest energy structure for each molecular ion form corresponds to the most abundant IMS band; that is, the lowest energy

structures are the most thermodynamically stable and appear with the larger relative abundance in the IMS spectra. Both deprotonated forms of FAD show more IMS bands than the protonated forms. Inspection of the $[M + H]^+$ molecular ion form of the deprotonated ($C_{27}H_{31}N_9O_{15}P_2$) FAD form shows that the main differences between the candidate structures proposed for the five IMS bands (A−E) are the distance and orientation between the adenine and isoalloxazine rings, where the deprotonation of the phosphate group near the adenine generates a resonance structure that stabilizes the π−π system between both rings. The $[M + Na]^+$ molecular ions of the
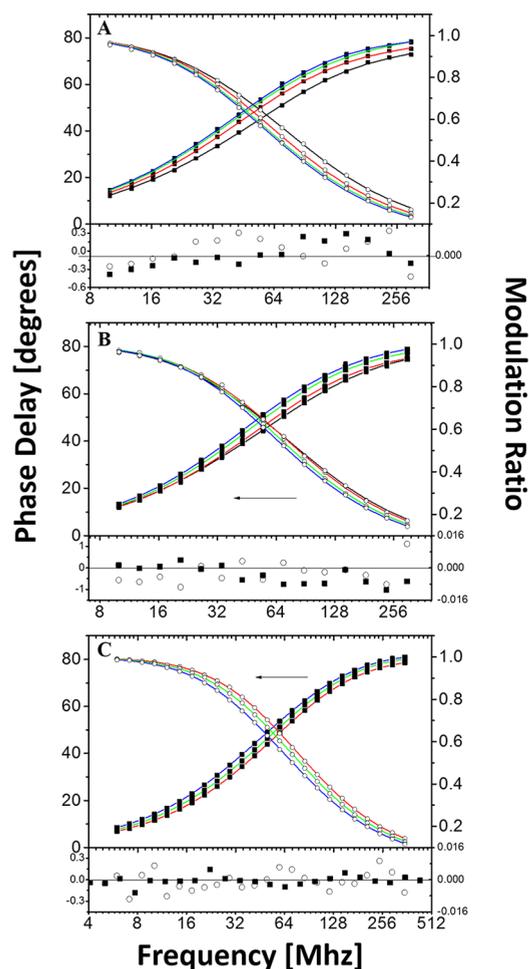
Figure 3. Frequency domain phase delay (solid squares) and modulation ratio (open circles) of 10 μM FAD in mixture of (A) ethanol−water and (B) methanol−water and (C) 10 μM FAD in mixture of ammonium acetate buffer−water as a function of the volume ratio of 0:100 (black line), 30:70 (red line), 50:50 (green line), and 70:30 (blue line). Solid lines represent the best fit to the data using a triple exponential decay.

deprotonated ($C_{27}H_{31}N_9O_{15}P_2$) FAD (F−H) form also showed the same orientation between both aromatic systems with an additional stabilization of the sodium ion present in the adduct. Moreover, the inspection of the $[M + H]^+$ molecular ion form of the protonated ($C_{27}H_{33}N_9O_{15}P_2$) FAD form shows that the main differences between the candidate structures proposed for the (I,J) IMS bands are the interaction between the ring systems without the stabilization provided by the resonance structure of the phosphate groups. The $[M + Na]^+$ molecular ions of the protonated ($C_{27}H_{33}N_9O_{15}P_2$) FAD form (K,L) also encounter the destabilization of the sodium ion present in the adduct. Inspection of the distances between the rings (4−6 Å) in the proposed candidate structures showed a good agreement with the solution experiments for the "stack" and "close" conformations, as well as previous reports.[54,56] A candidate structure for the "open" conformation will result in a CCS of 320 Å^2 (see structure in the Supporting Information), but no IMS band was experimentally observed. The latter suggests that solvation effects may equilibrate the "open" conformation in solution, while in the gas phase the ring interaction dominates and stabilizes in the "stack" and "close" conformations. Since the molar fraction of the "close" FAD conformation of ~270 ps lifetime is higher in the ethanol−water mixture compared to the methanol−ammonium acetate mixture or methanol−water mixture, we attribute the fraction of FAD with 270 ps lifetime to the larger CCSs conformations identified in IMS measurements (e.g., band H). Despite that different molecular ions are observed, inspection of the IMS spectra shows that mainly five IMS bands are detected (considering the expected CCS small shift between $[M + H]^+$ and $[M + Na]^+$ ions) but a direct correlation from the number of IMS bands to the number of fluorescence decay times is not possible. Moreover, the decay times can be related to the distances between the isoalloxazine and adenine ring. Inspection of the distances from the proposed candidate structures shows three main groups: 4.3 Å (conformer A), 4.8−5.6 Å (conformer B, C, D, F, G, H, I, J, K, and L), and 5.9 Å (conformer E). That is, the IMS experiments suggest that at least three decay times should be expected; however, differences between the distances of the three group of conformers can be too small to be resolved in lifetime measurements.[54,56]

Table 2. Fluorescence Decay Parameters Recovered for FAD in Ethanol−Water, Methanol−Water, and Methanol−Ammonium Acetate Mixtures[a]

	α_0	τ_0 (ns)	α_1	τ_1 (ns)	α_2	τ_2 (ns)	χ^2
water	0.28	0.27	0.50	2.43	0.23	4.62	1.02
EtOH−water (%)							
30−70	0.27	0.27	0.41	2.43	0.32	4.62	0.58
50−50	0.21		0.31		0.49		0.33
70−30	0.22		0.26		0.52		1.32
MetOH−water (%)							
30−70	0.19	0.36	0.71	2.45	0.09	4.25	1.33
50−50	0.22		0.68		0.10		2.84
70−30	0.20		0.66		0.14		1.18
MetOH−ammonium acetate (%)							
30−70	0.17	0.29	0.73	2.75	0.10	5.06	0.33
50−50	0.15		0.67		0.18		0.68
70−30	0.13		0.56		0.31		0.67

[a]Parameters were recovered using a triple exponential decay model. Decay lifetimes were set as linked variables. Errors of the recovered values were not shown but did not exceed 17% of their values.
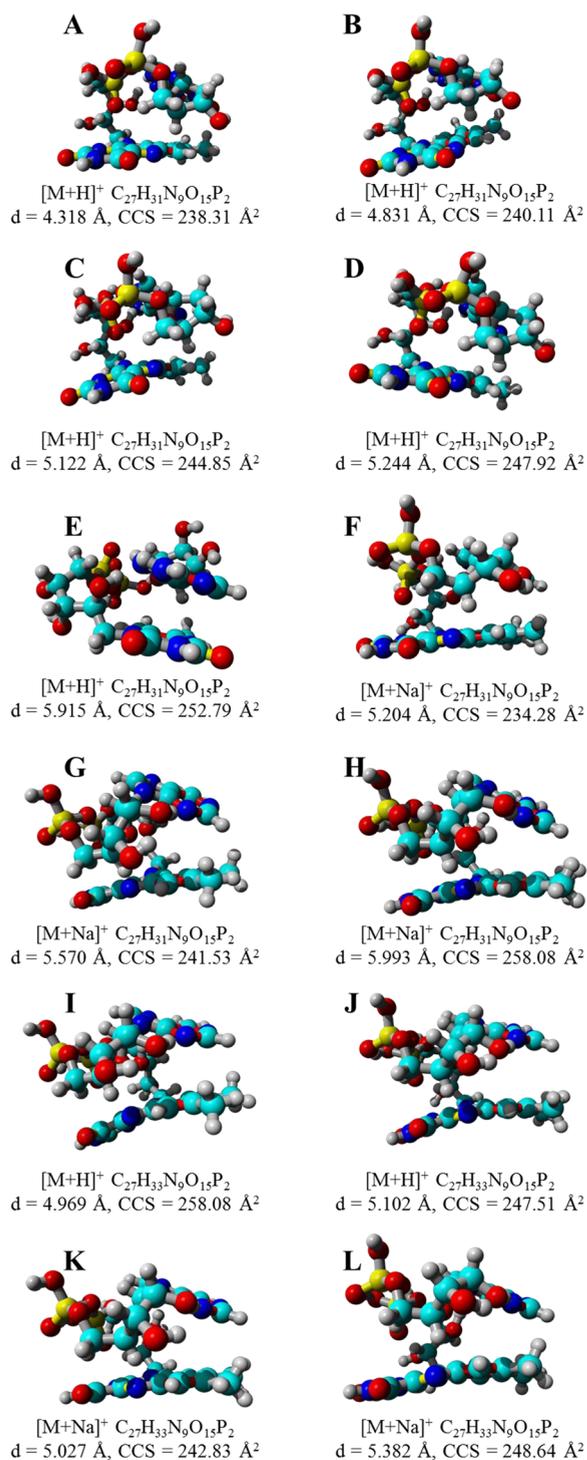
E

dx.doi.org/10.1021/ac5023666 | Anal. Chem. XXXX, XXX, XXX−XXX

A

[M+H]⁺ $C_2H_{31}N_9O_{15}P_2$
d = 4.318 Å, CCS = 238.31 Å²

B

[M+H]⁺ $C_{27}H_{31}N_9O_{15}P_2$
d = 4.831 Å, CCS = 240.11 Å²

C

[M+H]⁺ $C_{27}H_{31}N_9O_{15}P_2$
d = 5.122 Å, CCS = 244.85 Å²

D

[M+H]⁺ $C_{27}H_{31}N_9O_{15}P_2$
d = 5.244 Å, CCS = 247.92 Å²

E

[M+H]⁺ $C_{27}H_{31}N_9O_{15}P_2$
d = 5.915 Å, CCS = 252.79 Å²

F

[M+Na]⁺ $C_{27}H_{31}N_9O_{15}P_2$
d = 5.204 Å, CCS = 234.28 Å²

G

[M+Na]⁺ $C_{27}H_{31}N_9O_{15}P_2$
d = 5.570 Å, CCS = 241.53 Å²

H

[M+Na]⁺ $C_{27}H_{31}N_9O_{15}P_2$
d = 5.993 Å, CCS = 258.08 Å²

I

[M+H]⁺ $C_{27}H_{33}N_9O_{15}P_2$
d = 4.969 Å, CCS = 258.08 Å²

J

[M+H]⁺ $C_{27}H_{33}N_9O_{15}P_2$
d = 5.102 Å, CCS = 247.51 Å²

K

[M+Na]⁺ $C_{27}H_{33}N_9O_{15}P_2$
d = 5.027 Å, CCS = 242.83 Å²

L

[M+Na]⁺ $C_{27}H_{33}N_9O_{15}P_2$
d = 5.382 Å, CCS = 248.64 Å²

Figure 4. Candidate structures for the IMS bands observed for the [M + H]⁺ and [M + Na]⁺ molecular ions of the deprotonated (M = $C_{27}H_{31}N_9O_{15}P_2$) and protonated (M = $C_{27}H_{33}N_9O_{15}P_2$) FAD forms.

Figure 5. Typical IMS spectra of the [M + Na]⁺ ions of the protonated FAD form (M = $C_{27}H_{33}N_9O_{15}P_2$) as a function of the bath gas conditions. Notice the variation of the relative abundances of IMS bands as a function of the bath gas composition using ethanol, methanol, and acetonitrile as additives in the TIMS mobility cell.

The "solvation" and organic context effect on the number of FAD conformations was studied in the TIMS cell by using dopant gas additives (Figure 5). That is, each molecular ion conformation is isolated in the TIMS cell, and by introducing the dopant gas, we studied the influence of the collisional partner in the FAD conformational space in a single molecular ion−dopant molecule fashion. Inspection of Figure 5 shows that the interaction with the collision partner (electrostatic in nature) results in changes in the relative abundances of the
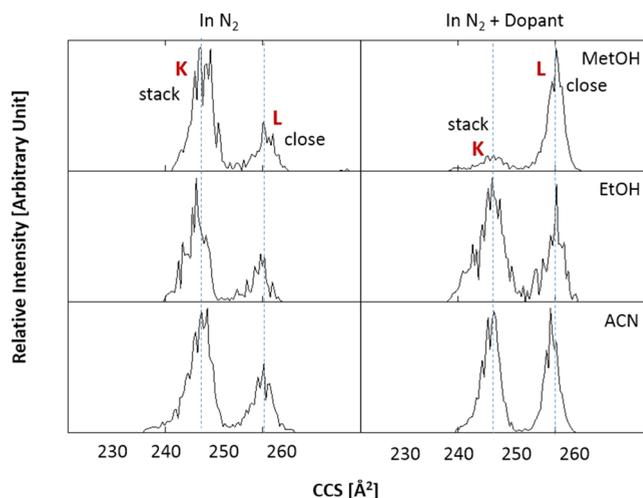
"stack" and "close" FAD conformers in the absence and presence of the dopant gas additives. That is, experiments suggest that, at the molecular level, the interaction with the organic molecules can induce the transition from "stack" to "close" conformations. Previous IMS studies have shown that different degrees of solvation are attainable as a function of the IMS experimental conditions and can be used (i) to increase IMS separation (e.g., drift tube, high field, and differential IMS analyzers[57−60]) and (ii) for structural assignments (e.g., determination of the solution state structures[28,29,36]). Polar molecules (e.g., methanol, ethanol, and acetonitrile) interact with ions very strongly via ion-dipole interactions (since they have a permanent dipole moment). Although changes in the IMS profile occurred with the dopant introduction (i.e., structure L and K relative abundances), the transition into the "open" conformation was not observed. The later suggest that a higher abundance of dopant molecules with respect to the bath gas is necessary to reach the FAD "open" state. Comparison between the solution and gas phase results suggest that the FAD solution state distribution can be preserved in the gas phase and gas-phase conformation-friendly conditions can be induced using dopant gases. Moreover, in both solution and gas phase, FAD three-dimensional structures are determined by the interplay between intramolecular interactions (e.g., $\pi-\pi$ system formed by the adenine and isoalloxazine rings) and interactions with the surrounding solvent/gas molecules. The workflow described here (TIMS-MS combined with MD using gas dopants) provides a powerful tool for the investigation of the gas phase "solvation" state of molecular ions.

■ CONCLUSIONS

In the current study, TIMS-MS combined fluorescence time decay and theoretical calculations were used to study FAD conformational space. Gas-phase experimental results showed that [M + H]⁺ and [M + Na]⁺ molecular ions are observed during ESI for the deprotonated ($C_{27}H_{31}N_9O_{15}P_2$) and protonated ($C_{27}H_{33}N_9O_{15}P_2$) FAD forms. For the first time, CCSs of 12 FAD conformations found by IMS experiments are reported and compared with theoretical calculations of candidate structures that correspond to the "stack" and

"close" conformations identified in solution by fluorescence lifetime measurements. The abundance of each conformer was consistent with their relative stability; that is, the larger intensity observed for a conformer corresponds to the most stable conformer. The examination of the conformational space generated by the candidate structures shows that the main motif that defines FAD conformational space is the interaction between the isoalloxazine and adenine groups. It was shown that the use of dopants in the TIMS cell permits the investigation of single molecular ion–dopant molecule interaction and can be used to study the gas-phase "solvation" state of biological molecules.

■ ASSOCIATED CONTENT

ⓢ Supporting Information

Additional information as noted in the text. This material is available free of charge via the Internet at http://pubs.acs.org.

■ AUTHOR INFORMATION

Corresponding Author

*Phone: 305-348-2037. Fax: 305-348-3772. E-mail: fernandf@fiu.edu.

Notes

The authors declare no competing financial interest.

■ ACKNOWLEDGMENTS

■ REFERENCES

(1) Amino, H.; Osanai, A.; Miyadera, H.; Shinjyo, N.; Tomitsuka, E.; Taka, H.; Mineki, R.; Murayama, K.; Takamiya, S.; Aoki, T.; Miyoshi, H.; Sakamoto, K.; Kojima, S.; Kita, K. *Mol. Biochem. Parasitol.* **2003**, *128*, 175.

(2) Braatsch, S.; Gomelsky, M.; Kuphal, S.; Klug, G. *Mol. Microbiol.* **2002**, *45*, 827.

(3) Bauer, C.; Elsen, S.; Swem, L. R.; Swem, D. L.; Masuda, S. *Philos. Trans. R. Soc., B* **2003**, *358*, 147.

(4) MacFarlane, A. W. t.; Stanley, R. J. *Biochemistry* **2003**, *42*, 8558–8568.

(5) van der Horst, M. A.; Hellingwerf, K. J. *Acc. Chem. Res.* **2004**, *37*, 13.

(6) Cosseau, C.; Garnerone, A. M.; Batut, J. *Mol. Plant-Microbe Interact.* **2002**, *15*, 598.

(7) Weber, G. *Biochem. J.* **1950**, *47*, 114.

(8) Barrio, J. R.; Tolman, G. L.; Leonard, N. J.; Spencer, R. D.; Weber, G. *Proc. Natl. Acad. Sci. U.S.A.* **1973**, *70*, 941.

(9) Weber, G.; Tanaka, F.; Okamoto, B. Y.; Drickamer, H. G. *Proc. Natl. Acad. Sci. U.S.A.* **1974**, *71*, 1264.

(10) Grininger, M.; Seiler, F.; Zeth, K.; Oesterhelt, D. *J. Mol. Biol.* **2006**, *364*, 561–566.

(11) Raszka, M.; Kaplan, N. O. *Proc. Natl. Acad. Sci. U.S.A.* **1974**, *71*, 4546.

(12) van den Berg, P. A. W.; Feenstra, K. A.; Mark, A. E.; Berendsen, H. J. C.; Visser, A. J. W. G. *J. Phys. Chem. US. B* **2002**, *106*, 8858.

(13) Nakabayashi, T.; Islam, M. S.; Ohta, N. *J. Phys. Chem. B* **2010**, *114*, 15254.

(14) Voet, D.; Rich, A. *Proc. Natl. Acad. Sci. U.S.A.* **1971**, *68*, 1151.

(15) Sarma, R. H.; Dannies, P.; Kaplan, N. O. *Biochemistry-US* **1968**, *7*, 4359.

(16) Sarma, R. H.; Mynott, R. J. *J. Am. Chem. Soc.* **1973**, *95*, 1641.

(17) Kainosho, M.; Kyogoku, Y. *Biochemistry-US* **1972**, *11*, 741.

(18) Kotowycz, G.; Teng, N.; Klein, M. P.; Calvin, M. *J. Biol. Chem.* **1969**, *244*, 5656.

(19) Valentine, S. J.; Counterman, A. E.; Clemmer, D. E. *J. Am. Soc. Mass. Spectrom.* **1999**, *10*, 1188.

(20) Kanu, A. B.; Dwivedi, P.; Tam, M.; Matz, L.; Hill, H. H. *J. Mass Spectrom.* **2008**, *43*, 1.

(21) Tao, L.; McLean, J. R.; McLean, J. A.; Russell, D. H. *J. Am. Soc. Mass. Spectrom.* **2007**, *18*, 1232.

(22) Ruotolo, B. T.; Benesch, J. L. P.; Sandercock, A. M.; Hyung, S.-J.; Robinson, C. V. *Nat. Protoc.* **2008**, *3*, 1139.

(23) Fernandez-Lima, F. A.; Blase, R. C.; Russell, D. H. *Int. J. Mass Spectrom.* **2010**, *298*, 111.

(24) Beveridge, R.; Chappuis, Q.; Macphee, C.; Barran, P. *Analyst.* **2013**, *138*, 32.

(25) Fenn, J.; Mann, M.; Meng, C.; Wong, S.; Whitehouse, C. *Science* **1989**, *246*, 64.

(26) Wyttenbach, T.; von Helden, G.; Bowers, M. T. *J. Am. Chem. Soc.* **1996**, *118*, 8355.

(27) Li, J.; Taraszka, J. A.; Counterman, A. E.; Clemmer, D. E. *Int. J. Mass Spectrom.* **1999**, *185–187*, 37.

(28) Kohtani, M.; Jarrold, M. F. *J. Am. Chem. Soc.* **2002**, *124*, 11148.

(29) Kohtani, M.; Breaux, G. A.; Jarrold, M. F. *J. Am. Chem. Soc.* **2004**, *126*, 1206.

(30) Hyung, S.-J.; Robinson, C. V.; Ruotolo, B. T. *Chem. Biol.* **2009**, *16*, 382.

(31) Fernandez-Lima, F. A.; Wei, H.; Gao, Y. Q.; Russell, D. H. *J. Phys. Chem. A* **2009**, *113*, 8221.

(32) Bush, M. F.; Hall, Z.; Giles, K.; Hoyes, J.; Robinson, C. V.; Ruotolo, B. T. *Anal. Chem.* **2010**, *82*, 9557.

(33) Pierson, N. A.; Chen, L.; Valentine, S. J.; Russell, D. H.; Clemmer, D. E. *J. Am. Chem. Soc.* **2011**, *133*, 13810.

(34) Zhong, Y.; Hyung, S.-J.; Ruotolo, B. T. *Expert Rev. Proteomics* **2012**, *9*, 47.

(35) Beveridge, R.; Chappuis, Q.; Macphee, C.; Barran, P. *Analyst* **2013**, *138*, 32.

(36) Silveira, J. A.; Fort, K. L.; Kim, D.; Servage, K. A.; Pierson, N. A.; Clemmer, D. E.; Russell, D. H. *J. Am. Chem. Soc.* **2013**, *135*, 19147.

(37) Chen, L.; Chen, S. H.; Russell, D. H. *Anal. Chem.* **2013**, *85*, 7826.

(38) Fernandez-Lima, F. A.; Kaplan, D. A.; Suetering, J.; Park, M. A. *Int. J. Ion Mobility Spectrom.* **2011**, *14*, 93.

(39) Fernandez-Lima, F. A.; Kaplan, D. A.; Park, M. A. *Rev. Sci. Instrum.* **2011**, *82*, 126106.

(40) Hernandez, D. R.; DeBord, J. D.; Ridgeway, M. E.; Kaplan, D. A.; Park, M. A.; Fernandez-Lima, F. *Analyst* **2014**, *139*, 1913.

(41) Schenk, E. R.; Ridgeway, M. E.; Park, M. A.; Leng, F.; Fernandez-Lima, F. *Anal. Chem.* **2014**, *86*, 1210.

(42) Schenk, E. R.; Mendez, V.; Landrum, J. T.; Ridgeway, M. E.; Park, M. A.; Fernandez-Lima, F. *Anal. Chem.* **2014**, *86*, 2019.

(43) Flanagan, L. A.; Hewlett-Packard Company. U.S. Patent 5872357, 1999.

(44) McDaniel, E. W.; Mason, E. A. *Mobility and diffusion of ions in gases*; John Wiley and Sons, Inc.: New York, 1973.

(45) Boens, N.; Qin, W.; Basarić, N.; Hofkens, J.; Ameloot, M.; Pouget, J.; Lefèvre, J.-P.; Valeur, B.; Gratton, E.; vandeVen, M.; Silva, N. D.; Engelborghs, Y.; Willaert, K.; Sillen, A.; Rumbles, G.; Phillips, D.; Visser, A. J. W. G.; van Hoek, A.; Lakowicz, J. R.; Malak, H.; Gryczynski, I.; Szabo, A. G.; Krajcarski, D. T.; Tamai, N.; Miura, A. *Anal. Chem.* **2007**, *79*, 2137.

(46) Frisch, M. J.; Trucks, G. W.; Schlegel, H. B.; Scuseria, G. E.; Robb, M. A.; Cheeseman, J. R.; Montgomery, J. A., Jr.; Vreven, T.; Kudin, K. N.; Burant, J. C.; Millam, J. M.; Iyengar, S. S.; Tomasi, J.; Barone, V.; Mennucci, B.; Cossi, M.; Scalmani, G.; Rega, N.; Petersson, G. A.; Nakatsuji, H.; Hada, M.; Ehara, M.; Toyota, K.; Fukuda, R.; Hasegawa, J.; Ishida, M.; Nakajima, T.; Honda, Y.; Kitao,

G

dx.doi.org/10.1021/ac5023666 | *Anal. Chem.* XXXX, XXX, XXX–XXX

O.; Nakai, H.; Klene, M.; Li, X.; Knox, J. E.; Hratchian, H. P.; Cross, J. B.; Bakken, V.; Adamo, C.; Jaramillo, J.; Gomperts, R.; Stratmann, R. E.; Yazyev, O.; Austin, A. J.; Cammi, R.; Pomelli, C.; Ochterski, J. W.; Ayala, P. Y.; Morokuma, K.; Voth, G. A.; Salvador, P.; Dannenberg, J. J.; Zakrzewski, V. G.; Dapprich, S.; Daniels, A. D.; Strain, M. C.; Farkas, O.; Malick, D. K.; Rabuck, A. D.; Raghavachari, K.; Foresman, J. B.; Ortiz, J. V.; Cui, Q.; Baboul, A. G.; Clifford, S.; Cioslowski, J.; Stefanov, B. B.; Liu, G.; Liashenko, A.; Piskorz, P.; Komaromi, I.; Martin, R. L.; Fox, D. J.; Keith, T.; Al-Laham, M. A.; Peng, C. Y.; Nanayakkara, A.; Challacombe, M.; Gill, P. M. W.; Johnson, B.; Chen, W.; Wong, M. W.; Gonzalez, C.; Pople, J. A. *Gaussian 03*, revision C.02; Gaussian, Inc.: Wallingford CT, 2004.

(47) Mesleh, M. F.; Hunter, J. M.; Shvartsburg, A. A.; Schatz, G. C.; Jarrold, M. F. *J. Phys. Chem.* **1996**, *100*, 16082.

(48) Shvartsburg, A. A.; Jarrold, M. F. *Chem. Phys. Lett.* **1996**, *261*, 86.

(49) Kim, H. I.; Kim, H.; Pang, E. S.; Ryu, E. K.; Beegle, L. W.; Loo, J. A.; Goddard, W. A.; Kanik, I. *Anal. Chem.* **2009**, *81*, 8289.

(50) Campuzano, I.; Bush, M. F.; Robinson, C. V.; Beaumont, C.; Richardson, K.; Kim, H.; Kim, H. I. *Anal. Chem.* **2011**, *84*, 1026.

(51) Singh, U. C.; Kollman, P. A. *J. Comput. Chem.* **1984**, *5*, 129.

(52) Besler, B. H.; Merz, K. M.; Kollman, P. A. *J. Comput. Chem.* **1990**, *11*, 431.

(53) Larriba, C.; Hogan, C. J., Jr. *J. Phys. Chem. A* **2013**, *117*, 3887.

(54) Sengupta, A.; Singh, R. K.; Gavvala, K.; Koninti, R. K.; Mukherjee, A.; Hazra, P. *J. Phys. Chem. B* **2014**, *118*, 1881.

(55) Radoszkowicz, L.; Huppert, D.; Nachliel, E.; Gutman, M. *J. Phys. Chem. A* **2009**, *114*, 1017.

(56) Ross, S. K.; McDonald, G.; Marchant, S. *Analyst* **2008**, *133*, 602.

(57) Sengupta, A.; Khade, R. V.; Hazra, P. *J. Photochem. Photobiol., A* **2011**, *221*, 105.

(58) Eiceman, G. A.; Krylov, E. V.; Krylova, N. S.; Nazarov, E. G.; Miller, R. A. *Anal. Chem.* **2004**, *76*, 4937.

(59) Fernández-Maestre, R.; Wu, C.; Hill, H. H. *Rapid Commun. Mass Spectrom.* **2012**, *26*, 2211.

(60) Dwivedi, P.; Wu, C.; Matz, L. M.; Clowers, B. H.; Siems, W. F.; Hill, H. H., Jr. *Anal. Chem.* **2006**, *78*, 8200.